Large Single Crystals of Graphene on Melted Copper Using Chemical Vapor Deposition

Yimin A. Wu,[†] Ye Fan,[†] Susannah Speller,[†] Graham L. Creeth,[‡] Jerzy T. Sadowski,[§] Kuang He,[†] Alex W. Robertson,[†] Christopher S. Allen,[†] and Jamie H. Warner[†,*]

[†]Department of Materials, University of Oxford, Parks Road, Oxford, OX1 3PH, United Kingdom, [‡]School of Physics & Astronomy, University of Leeds, Leeds LS2 9JT, United Kingdom, and [§]Center for Functional Nanomaterials, Brookhaven National Laboratory, Upton, New York 11973, United States

ABSTRACT

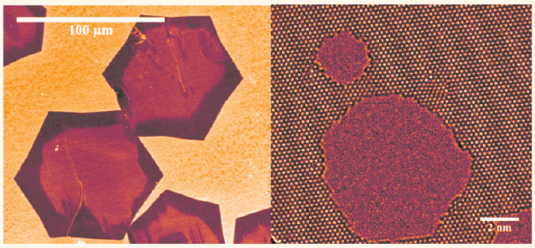

A simple method is presented for synthesizing large single crystal graphene domains on melted copper using atmospheric pressure chemical vapor deposition (CVD). This is achieved by performing the reaction above the melting point of copper (1090 °C) and using a molybdenum or tungsten support to prevent balling of the copper from dewetting. By controlling the amount of hydrogen during growth, individual single crystal domains of monolayer graphene greater than 200 μm are produced within a continuous film. Stopping growth before a complete film is formed reveals individual hexagonal domains of graphene that are epitaxially aligned in their orientation. Angular resolved photoemission spectroscopy is used to show that the graphene grown on copper exhibits a linear dispersion relationship and no sign of doping. HRTEM and electron diffraction reveal a uniform high quality crystalline atomic structure of monolayer graphene.

KEYWORDS: CVD · graphene · large crystal · copper

The key challenge for implementing graphene in applications is the ability to routinely fabricate large single crystal graphene domains within a continuous 2D film. Chemical vapor deposition (CVD) using copper as a metal catalyst is a promising route toward this goal.[1−8] However, the quality for graphene grown by CVD is generally not as good as those exfoliated from graphite because of the small grain size and thus high amount of grain boundaries and defects.[9−12] Improving the size of graphene domains is generally achieved by reducing the number of nucleation sites.[13] Recent work has shown that preparation of the copper surface is crucial to reducing nucleation sites.[13,14] The nucleation sites are often associated with surface roughness, impurities, and copper grain boundaries.[15] Electropolishing of the copper foils has been shown to improve the size of graphene domains.[14] Large-sized graphene domains have been grown using low-pressure CVD by adopting the parcel approach, where a copper foil is folded into a small parcel to reduce the amount of methane entering and also provide a better environment for growth.[2] The large graphene domains grown by this method adopt a flower-like shape. Ideally it would be beneficial to grow large domains with hexagonal geometry, rather than flower geometry, as these are known to be single crystal, and will have more uniform edge termination of the graphene lattice.[3−8] This is important when considering the interface of graphene domains, which will be more complicated when two flower shaped domains connect as compared to two hexagonal domains.[6]

An alternative method of obtaining graphene domains with increased size has been to use graphene seeds as preformed nucleation sites.[5,6] This was achieved by first growing graphene using conventional CVD methods on copper, then using lithography to pattern seeds at regular intervals. While this is a powerful method of control, it requires substantially more effort and time to obtain larger domain graphene as compared to a one-step direct growth on copper foil approach.

Here we present a simple one-step method to grow graphene on copper with single crystal sizes exceeding 200 μm. This is achieved by performing the growth at 1090 °C, whereby the copper melts and forms a liquid state. Since the growth of graphene on copper is

* Address correspondence to Jamie.warner@materials.ox.ac.uk.

Received for review February 7, 2012 and accepted May 15, 2012.

Published online May 22, 2012
10.1021/nn3016629

primarily a surface driven process, it does not require it to be in a solid form. We show that control of the supplied hydrogen during growth is essential for large graphene crystal sizes, indicating that it plays a major role in the catalytic process of graphene formation.[16] We have explored a wide range of parameters and here we present the key synthesis details we have developed that lead to desirable very large domain graphene.

RESULTS AND DISCUSSION

To obtain and maintain a flat copper surface when melted, a molybdenum foil support was used. This prevented balling of the copper that occurs if the reaction is performed on quartz, silicon, or other nonwetting supports, shown schematically in Figure 1a,b. Figure 1c shows a photo of the sample after such a procedure with the copper well spread across the Mo supporting film.

After exploring a wide range of experimental parameters, we found that using a flow rate of 80 sccm of hydrogen and 10 sccm of CH_4 led to the best results in terms of producing monolayer graphene. Reducing the flow rate of hydrogen led to faster growth rates, but thicker films (see Supporting Information). After 15 min of growth time with 80 sccm of hydrogen, the reaction was stopped, and this resulted in well-defined hexagonal graphene domains (shown in Figures 2a,b plus the inset in 2b). The nucleation density was low and this enabled large domains to grow. Two different size ranges are observed; large domains greater than 100 μm and smaller domains between 20 and 40 μm. Surprisingly, the hexagonal domains were aligned in their orientation. For 15 min growth a continuous film was not produced, only isolated domains. Figure 2 panels c and d show SEM images of the graphene after 45 min of growth, and a continuous film was observed. Figures 2 panels e and f show the SEM images for 90 min of growth, and a continuous film was also produced. The major difference between the 45 and 90 min growth samples is that the 90 min growth showed less contrast variation in SEM, which may indicate more uniform layer coverage or reduced amounts of amorphous carbon on the surface. The SEM images in Figures 2c–f were intentionally taken in regions near the edge of the copper where the graphene films had ruptured or not fully covered to the edge, so that some contrast can be observed in the images. For 45 and 90 min of growth more than 90% of the copper is covered with a continuous film, with only the edges of the copper deviating. Samples can be easily trimmed around the edges to remove these broken to leave a fully continuous 2D film of graphene. Figure 2g shows a high magnification SEM image of the fully continuous region of the graphene film. Color is used to highlight the variation in contrast that arises due to changes in the number of graphene layers.

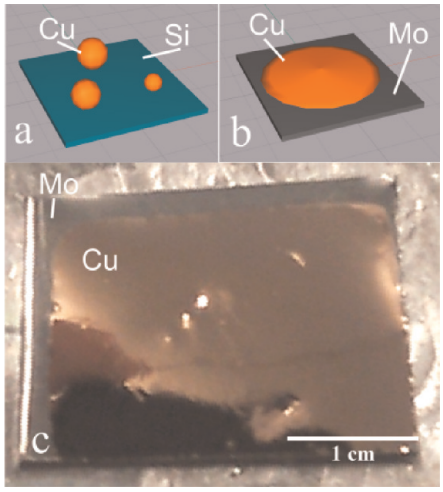

Figure 1. Schematic illustrations showing (a) balling of copper on silicon and (b) flat thin film of copper on molybdenum, after heating to melted phase (1090 °C and cooling). (c) Photo of thin copper film on a molybdenum support after heating to melted phase and cooling.

Lines of contrast associated with wrinkles in graphene due to cooling are observed. Apart from the wrinkles, the overall contrast of the graphene is uniform.

Raman spectroscopy was performed on these three films and is shown in Figures 3 panels a, b, and c for growth times of 15, 45, and 90 min, respectively. Figure 3a shows a 2D:G ratio that is less than 1 and indicates the hexagonal domains are likely to be more than one layer. Figures 3 panels b and c show a 2D:G ratio greater than 1, indicating the graphene is between 1 and 2 layers. Further evidence will in fact show that the 90 min growth time (Figure 2g) is monolayer graphene, and we focused our attention on characterizing this sample in depth. We performed 2D Raman spectroscopy mapping of the sample grown for 90 min and extracted the intensity ratio of the 2D:G peaks as a figure of merit for the number of graphene layers. Figure 3d shows a 2D Raman map of graphene on the copper after 90 min growth at 1090 °C taken over a $100 \times 100\ \mu m^2$ area, in steps of 4 μm. Figure 3e shows a similar 2D map of 2D:G ratio after transferring onto a SiO_2/Si substrate, over a $200 \times 200\ \mu m^2$ area with 8 μm steps. A typical Raman spectrum of the graphene on the SiO_2/Si substrate is presented in Figure 3f. The 2D Raman maps show that the 2D/G ratio is greater than 1 (red or green) for the majority of the sample, indicating that more than 90% of the sample is monolayer over this vast region.[17]

Further evidence that the graphene produced from 90 min of growth was monolayer was obtained by directly imaging the atomic structure using the Oxford-JEOL-2200MCO FEG C_s aberration-corrected HRTEM at an accelerating voltage of 80 kV. The clean transferred (clean transfer method provided in Supporting Information) graphene on Si_3N_4 (denoted SiN) TEM grids that contained an array of 2.5 μm holes is shown in the optical image in

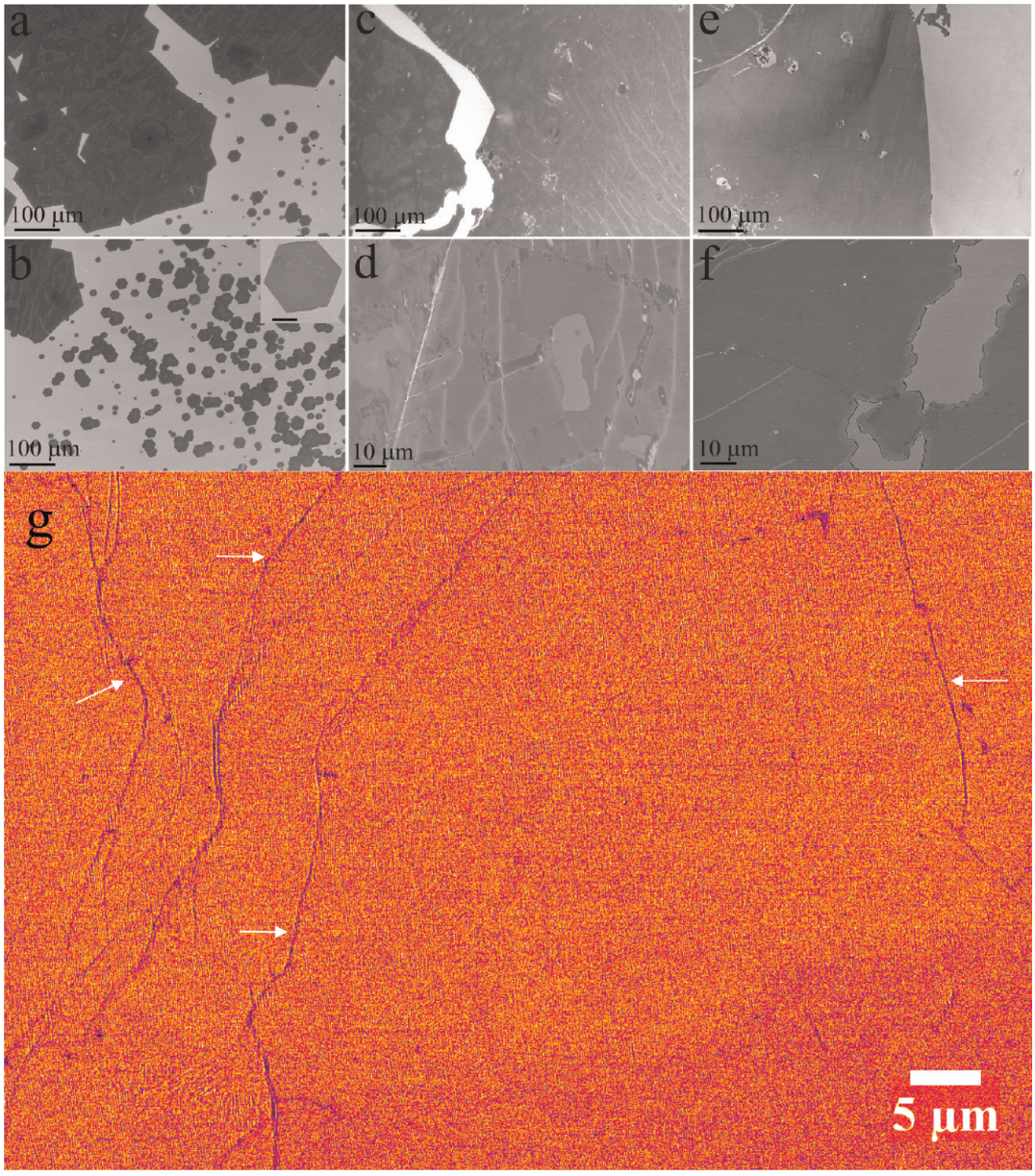

Figure 2. SEM images of graphene produced with 80 sccm hydrogen flow rate for growth times of (a–b) 15 min (inset shows hexagonal graphene domain with 20 μm scale bar), (c–d) 40 min, and (e–f) 90 min. (g) High magnification SEM image of graphene on copper produced with 90 min growth time. Color is used to highlight contrast variation. Arrows indicate typical wrinkles in the graphene film.

Figure 4a. Figure 4b shows a low magnification TEM image of the holes with labeling of X, Y and Z axis to form a labeling system for identification of specific holes within the grid. Focused electron beam irradiation is known to open up holes in graphene layers, one by one, enabling the counting of layers. We found that all the graphene examined using HRTEM was purely monolayer, with no signs of small extra bilayer layers that are often found in the CVD growth of graphene with solid copper catalysts. Figure 4c shows a HRTEM image of a typical region of graphene with two holes sputtered by electron beam irradiation. These holes directly open to vacuum and show that the graphene is monolayer. The small disorder in the graphene film is caused by the electron beam irradiation and is not intrinsic to the film. During our extensive HRTEM investigation of more than 50 individual 2 μm windows in the TEM grid, we found no signs of noticeable grain boundaries or any intrinsic large scale defects or disorder. To elucidate the typical crystallite size within the 2D film we measured the selected area electron diffraction (SAED) pattern from graphene along 45 consecutive windows of the TEM grid in the *x*-axis direction, starting from the 0 point in Figure 4b. Figure 4d shows the SAED patterns for several hole windows, numbered in the top left of each panel (*i.e.*, x1 corresponds to hole 1 along the *x* axis) The relative angle in degrees, θ, of the graphene lattice was measured from

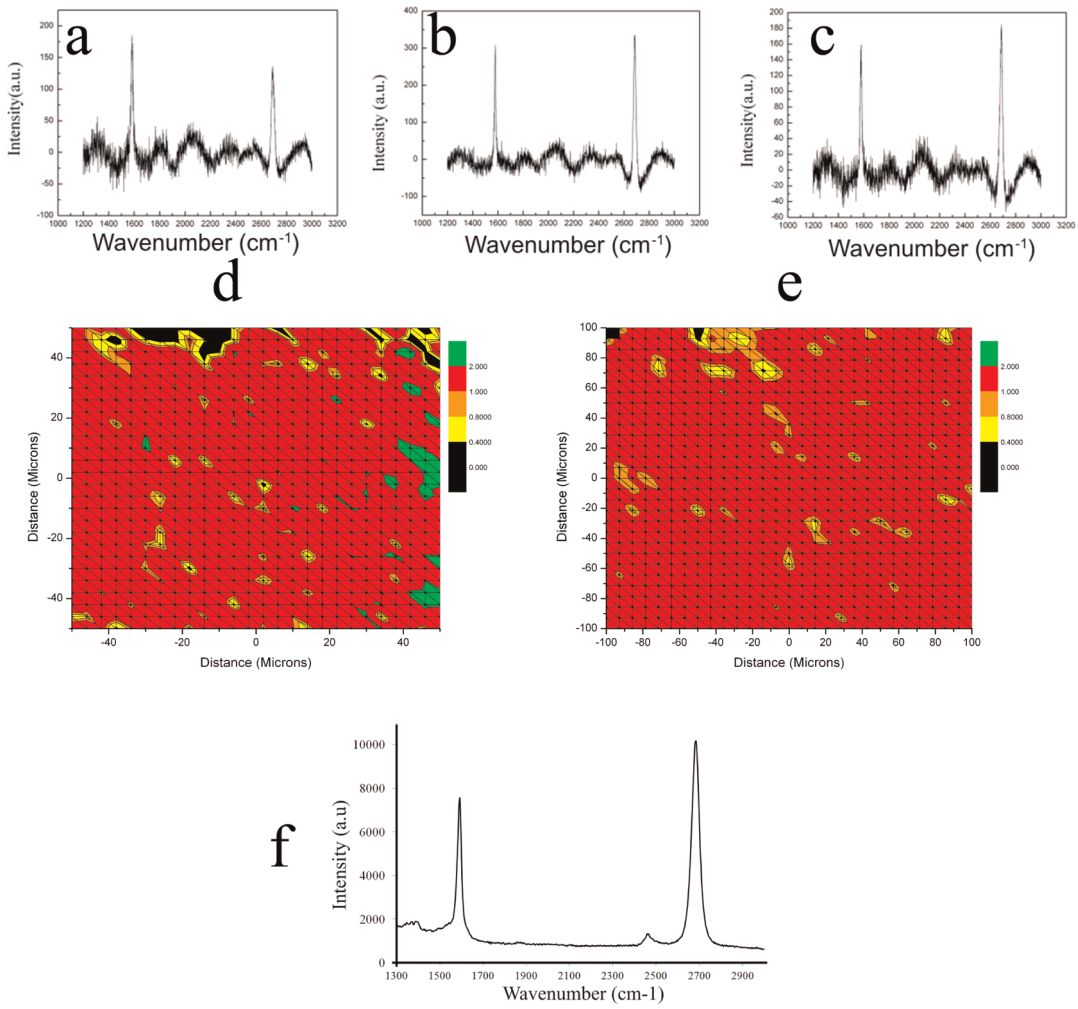

Figure 3. Raman spectra taken on copper after growth times of (a) 15 min, (b) 40 min, and (c) 90 min, (copper background subtracted for all spectra). (d) 2D map (100 μm $\times$ 100 μm, 4 μm step) of the 2D:G peak ratio for graphene grown for 90 min at 1090 °C on copper. (e) 2D map (200 μm $\times$ 200 μm, 8 μm step) of the 2D:G intensity ratio for graphene grown for 90 min at 1090 °C and then transferred onto a SiO_2/Si substrate. (f) Typical Raman spectrum of graphene grown for 90 min at 1090 °C and then transferred onto a SiO_2/Si substrate.

the SAED, as shown in the x0 plane in Figure 4d, and is marked in the bottom left of each panel. All SAED patterns were single crystal. Less than 2° rotation of the graphene lattice direction is measured between x0 and x18, which corresponds to a distance of 81 μm. Between x18 and x22, a step increase of 3° occurs, which correlated with a slight pinching of the film on the SiN grid. Overall a lattice rotation of less than 5° occurs between x0 and x45, which corresponds to a distance of $\sim$202 μm. Similar measurements were taken for windows in the *y* and *z* axes, both which showed similar orientations. The limitation of the measurements was that x45 was the last hole in the TEM grid. These results show a remarkable 200 μm single crystal of monolayer graphene has been produced. Analysis of the intensity of the SAED spots as a function of tilt angle also confirmed the graphene was monolayer and not bilayer (see Supporting Information).

We next used microspot angle-resolved photoemission spectroscopy (micro-ARPES) to examine the graphene on copper produced by the 90 min growth time, prior to transfer. The measurements have been performed at XPEEM/LEEM endstation, at National Synchrotron Light Source beamline U5UA. Data were taken with an incident photon energy of 43 eV. Figure 5a shows detected intensity in the k_x-k_y plane, at an energy 0.7 eV below the Fermi energy, E_F, and Figure 5b shows the $E(k)$ intensity close to the K point, along a line perpendicular to $\Gamma-K$, indicated in Figure 5a. The presence of multiple sets of features shown in the micro-ARPES intensity map in Figure 5a is attributed to terracing of the copper surface and subsequent deviation of the graphene lattice. Figure 5b shows a single, linear dispersion relationship close to E_F, indicating monolayer graphene and no sign of doping. This confirms that the graphene is of high quality, and that, despite the epitaxial nature of the growth, there is little electronic interaction with the substrate. Further from E_F the structure is more difficult to ascertain due to contributions from both of the tilted domains.

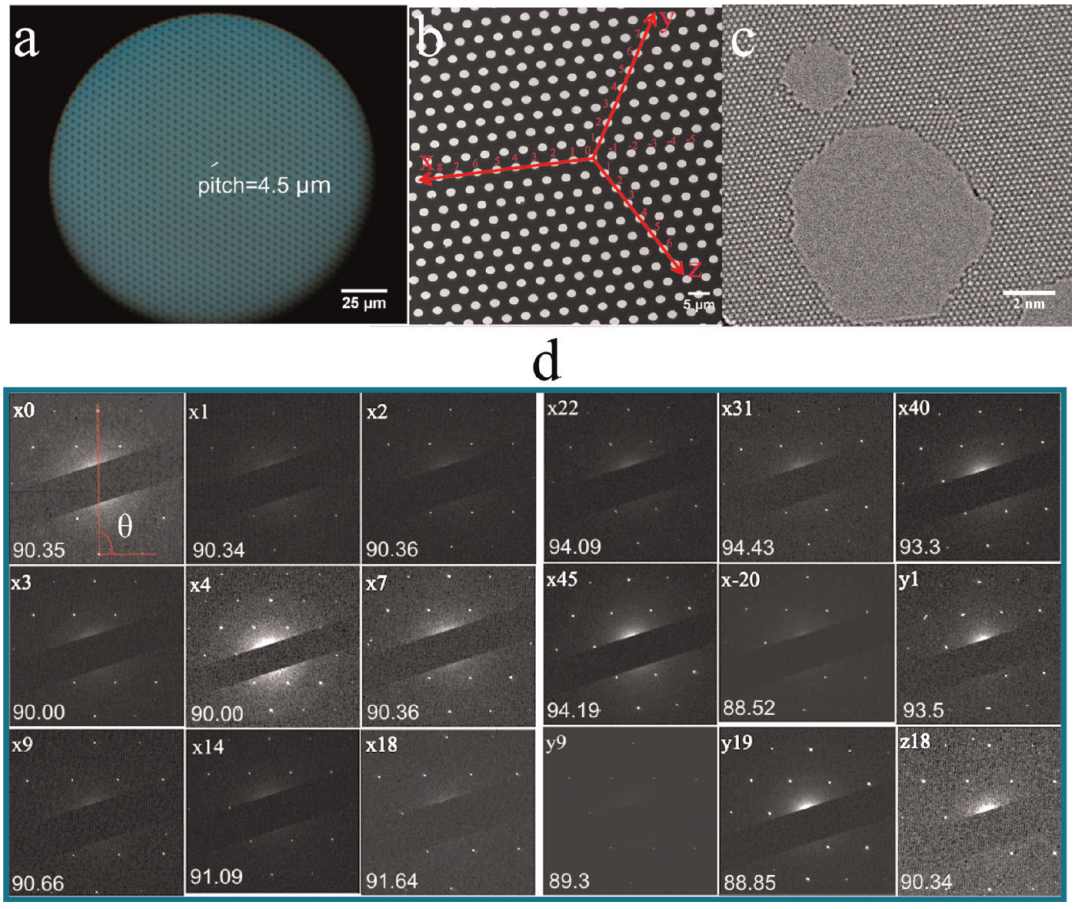

Figure 4. (a) Optical image of a SiN TEM grid with array of 2.5 μm window holes. (b) Low magnification TEM image of the SiN TEM grid with array of 2 μm window holes. (c) Aberration-corrected HRTEM image of graphene on SiN grid after prolonged electron beam irradiation to count the number of layers by hole opening. (d) Selected area electron diffraction patterns taken from different regions of the SiN TEM grid, labeled (top left in each panel) according to the *X*, *Y*, *Z* axis scheme indicated in panel. Measured angle (in degrees) of graphene lattice is recorded in bottom left of each panel, according to the axis defined in the first (x0) panel.

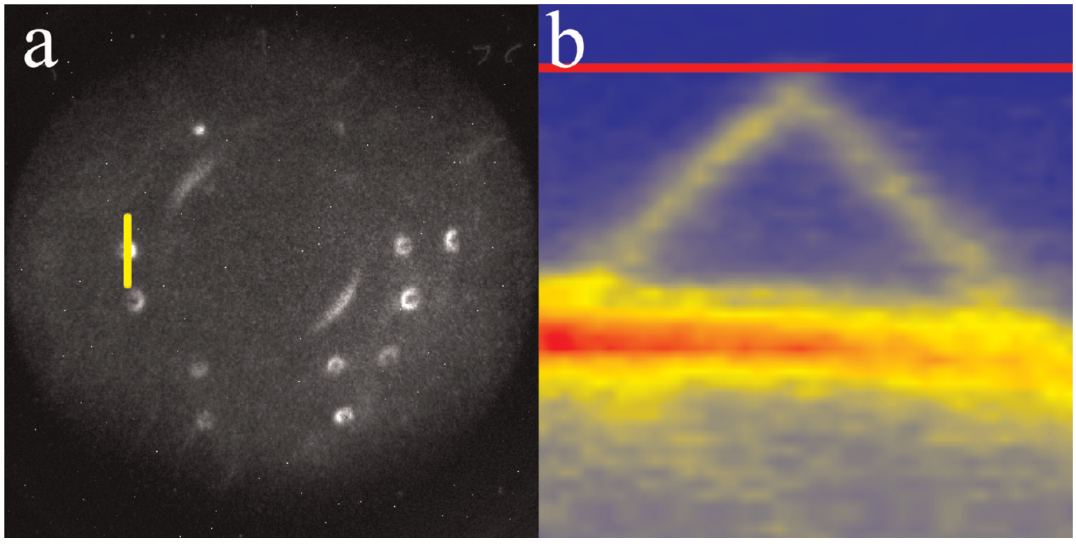

Figure 5. (a) Detected intensity in the k_x-k_y plane, at an energy 0.9 eV below the Fermi energy, E_F. (b) $E(k)$ intensity close to *K* point, along a line perpendicular to $\Gamma-K$ (indicated by the yellow line in panel a), with the Fermi energy represented by the red line.

We use electron backscattered diffraction (EBSD) to examine the crystallographic nature of the copper beneath the graphene after growth. Electron backscatter diffraction analysis on the copper substrate

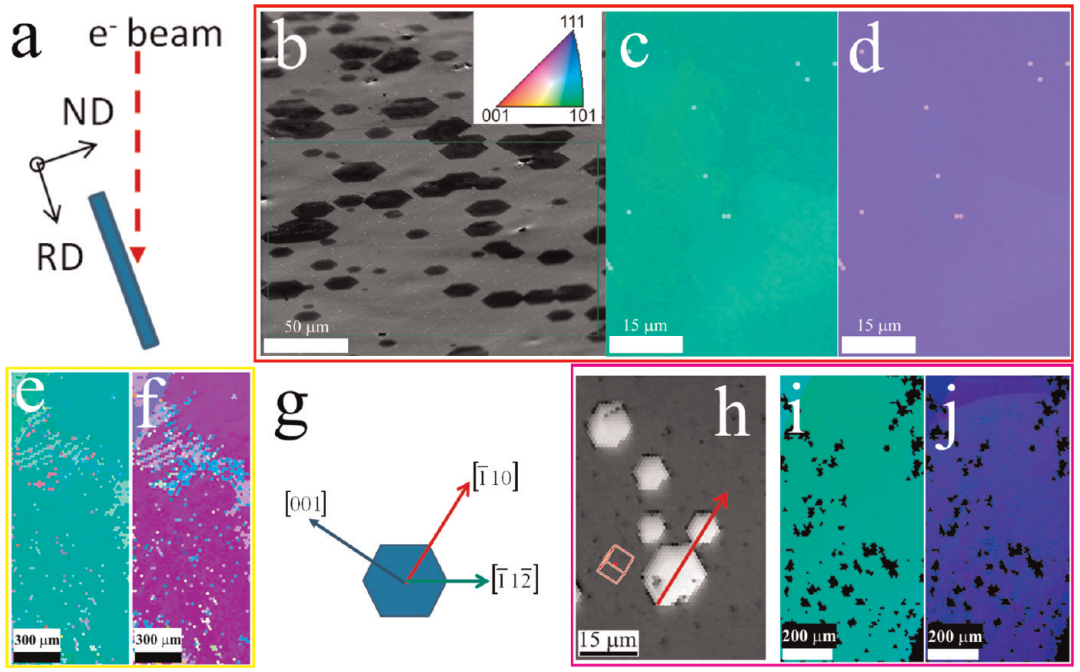

Figure 6. (a) Schematic showing the angle of the electron beam relative to the sample, with the normal direction (ND) and in-plane direction (RD). (b) SEM image of graphene on copper after 15 min growth. Inset shows color codex used for labeling copper lattice directions for electron backscattered diffraction (EBSD) maps. EBSD maps showing (c) ND of copper lattice and (d) RD of copper lattice. Larger EBSD maps showing (e) ND of copper lattice and (f) RD of copper lattice. (g) Diagram showing orientation of copper lattice with respect to the hexagonal-shaped graphene domain. (h) SEM image showing hexagonal graphene domains with a red arrow indicating a copper ⟨110⟩ lattice direction. The red cube shows the orientation of the underlying copper unit cell. EBSD maps for graphene with 90 min growth time, showing (i) ND of copper lattice and (j) RD of copper lattice.

was carried out using TSL software in a JEOL JSM 6500F FEGSEM. Figure 6a is a schematic showing the angle of the electron beam relative to the sample and the normal direction (ND) and in-plane direction (RD). In our reactions, the copper reaches some form of molten state and then rapid cooling leads to crystallization. Figure 6b shows a SEM image (tilted by 70°) of sample with 15 min growth time, as in Figure 2a,b, with aligned graphene hexagons. The inset in the top right shows the color codex used to display copper lattice directions in the EBSD maps. Figure 6 panels c and d are 2D EBSD maps showing the crystallographic orientation of the copper lattice along the sample normal direction (ND) and an in-plane direction (RD), taken from the boxed region in Figure 6b. Figure 6c shows that the copper has a {110} surface, and Figure 6d shows that there are no in-plane rotations and the copper is a large single crystal. Figure 6panels e and f present similar measurements, (*i.e.*, ND and RD, respectively), but over a substantially larger area of copper for the 15 min growth time. This reveals that upon cooling the melted copper forms a big single crystal structure with ({110} surface. Using the EBSD map in Figure 6c in conjunction with the SEM image in Figure 6b enables the relative orientation of the copper lattice with respect to the hexagonal-shaped graphene domain to be determined, shown schematically in Figure 6g. Figure 6h shows an EBSD image quality map which clearly shows the hexagonal graphene domains (presumably because the graphene layer protects the Cu surface from environmental damage which reduces the quality of the EBSD patterns) with the red arrow indicating the [$\bar{1}$10] copper lattice direction and the red cube showing the orientation of the underlying copper unit cell. It has been shown that the edges of hexagonal graphene domains correspond to the zigzag direction in the graphene lattice.[6] This then provides correlation between the graphene lattice direction and the copper lattice direction. Finally we analyzed the EBSD maps of graphene grown for 90 min to see whether there is a change in the copper crystallography. Figure 6 panels i and j show the ND and RD EBSD maps for the 90 min growth time. This shows that a similar (110) copper surface and large single crystal structure is obtained. Some twinning of the copper lattice was observed, and this also resulted in the rotation of the orientation of the graphene hexagons grown for 15 min. This indicates the alignment is driven purely by the epitaxial relationship with the copper lattice and not from other mechanisms such as gas flow.

To show that the hexagonal domains of graphene produced after 15 min of growth were aligned, Figure 7a presents a SEM image of a region showing more than 50 domains over a region 750 μm × 500 μm. A histogram plotting the frequency count for measured orientation angles of more than 50 hexagonal domains

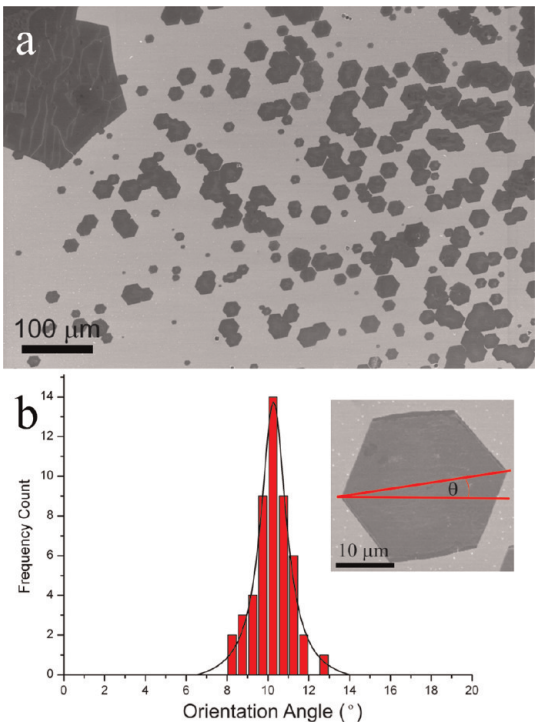

Figure 7. (a) SEM image of a region showing more than 50 domains over a region 750 μm $\times$ 500 μm. (b) A histogram plotting the frequency count for measured orientation angles of more than 50 hexagonal domains. A Lorentzian distribution fits the data well, black curve, giving a center point of 10.27°, and a width of 1.53°. The inset in panel b illustrates the orientation angle, θ, relative to the horizontal used for the histogram.

is presented in Figure 7b. The inset in Figure 7b illustrates the orientation angle, θ, relative to the horizontal used for the histogram. A Lorentzian distribution fits the data well, (black curve in Figure 7b), giving a center point of 10.27° and a width of 1.53°. Statistical analysis of the data set gives an average orientation angle of 10.2 $\pm$ 0.9°, which corresponds to a $\sim$ 9% standard deviation in the orientation angle of more than 50 hexagonal graphene domains. This confirms the tight alignment over distance scales exceeding 500 μm.

The alignment of the graphene domains means that the atomic lattice is orientated as well. This then prompts the discussion about the merger of multiple domains to form one larger graphene crystal. If two graphene domains are aligned in their lattice orientation and merge together during growth they will then become a single crystalline domain. The interface where the two domains merge together may contain defects and disorder if the alignment is not exact or the atomic stitching processes are flawed. But it is also possible that significant defects and disorder may not occur if the alignment between domains is excellent. During our extensive HRTEM search we could not find regions of significant disorder that might be associated with the interface where two aligned graphene domains merged together.

CONCLUSION

The results presented here show a simple method for obtaining large 200 μm single crystals of monolayer graphene within a continuous film. No fancy pretreatment of the copper is needed, nor do special seed sites need to be created. This approach can be easily applied by the large number of groups that currently produce graphene on copper using CVD. It is surprising that hexagonal graphene domains produced after 15 min of growth were aligned in their orientation. The EBSD indicated an epitaxial relationship between the copper surface and the graphene, but since the copper is in a liquid state during the addition of methane, this suggests a fairly complex growth model. The epitaxial alignment of graphene domains provides a means for rapidly fabricating large single crystals from multiple domains and may be a key step toward wafer-scale single crystals of monolayer graphene.

EXPERIMENTAL SECTION

Graphene CVD Synthesis. The copper foil (99.999% purity, 0.1 mm thick, Alfa Aesar) is placed on a Mo or W support (0.1 mm thick) and positioned in a 1 in. quartz tube within a horizontal furnace. It is then heated up to 1090 °C under argon flow (200 sccm) and then reduced in hydrogen (100 sccm) (1:3 H_2/Ar mix) at 1090 °C for 30 min. Then the flow rate of hydrogen during growth was adjusted among 10, 40, and 80 sccm. After this, CH_4 (10 sccm of 1:99 CH_4/Ar mix) was added for a desired period of growth time, which was adjusted among 15, 45, and 90 min. After the reaction in CH_4, the samples were rapidly cooled by being removed from the hot zone of the furnace and allowed to cool to room temperature.

Conflict of Interest: The authors declare no competing financial interests.

Acknowledgment. Y. Wu is grateful for financial support from the EPSRC International Doctoral Scholarship (IDS), Wolfson China Scholarship, China Oxford Scholarship Fund, and Overseas Research Scholarship. J. Warner is grateful for the support from the Royal Society and Balliol College. Research carried out in part at the Center for Functional Nanomaterials and National Synchrotron Light Source, Brookhaven National Laboratory, is supported by the U.S. Department of Energy, Office of Basic Energy Sciences, under Contract No. DE-AC02-98CH10886.

Supporting Information Available: (1) Clean transfer of graphene to SiN TEM grids; (2) variation in graphene growth by reducing hydrogen flow rate; (3) variation in graphene growth by increasing argon gas flow rate; (4) copper lattice orientation relative to the hexagonal-shaped graphene domains; (5) using e-beam sputtering and direct imaging of the graphene lattice to distinguish monolayer from multilayer graphene; (6) analysis of the selected area electron diffraction pattern as a function of tilt angle; (7) optical contrast of graphene transferred onto Si:SiO_2 substrates; (8) comparison of molten Cu and solid-state Cu catalysts. This material is available free of charge *via* the Internet at http://pubs.acs.org.

REFERENCES AND NOTES

1. Li, X.; Cai, W.; An, J.; Kim, S.; Nah, J.; Yang, D.; Piner, R.; Velamakanni, A.; Jung, I.; Tutuc, E.; *et al*. Large Area Synthesis of High Quality and Uniform Graphene Films on Copper Foils. *Science* **2009**, *324*, 1312–1314.
2. Li, X.; Magnuson, C. W.; Venugopal, A.; Tromp, R. M.; Hannon, J. B.; Vogel, E. M.; Colombo, L.; Ruoff, R. S. Large-Area Graphene Single Crystals Grown by Low-Pressure Chemical Vapor Deposition of Methane on Copper. *J. Am. Chem. Soc.* **2011**, *133*, 2816–2819.
3. Yan, K.; Peng, H.; Zhou, Y.; Li, H.; Liu, Z. Formation of Bilayer Bernal Graphene: Layer-by-Layer Epitaxy *via* Chemical Vapor Deposition. *Nano Lett.* **2011**, *11*, 1106–1110.
4. Wu, B.; Geng, D.; Guo, Y.; Huang, L.; Xue, Y.; Zheng, J.; Chen, J.; Yu, G.; Liu, Y.; Hu, W. Equiangular Hexagon-Shape-Controlled Synthesis of Graphene on Copper Surface. *Adv. Mater.* **2011**, *23*, 3522–3525.
5. Wu, W.; Jauregui, L. A.; Su, Z.; Liu, Z.; Bao, J.; Chen, Y. P.; Yu, Q. K. Growth of Single Crystal Graphene Arrays by Locally Controlling Nucleation on Polycrystalline Cu Using Chemical Vapor Deposition. *Adv. Mater.* **2011**, *23*, 4898–4903.
6. Yu, Q. K.; Jauregui, L. A.; Wu, W.; Colby, R.; Tian, J.; Su, Z.; Cao, H.; Liu, Z.; Pandey, D.; Wei, D.; *et al*. Control and Characterization of Individual Grains and Boundaries in Graphene Grown by Chemical Vapour Deposition. *Nat. Mater.* **2011**, *10*, 443–449.
7. Robertson, A. W.; Warner, J. H. Hexagonal Single Crystal Domains of Few Layer Graphene on Copper Foils. *Nano Lett.* **2011**, *11*, 1182–1189.
8. Wu, Y. A.; Robertson, A. W.; Schäffel, F.; Speller, S. C.; Warner, J. H. Aligned Rectangular Few-Layer Graphene Domains on Copper Surfaces. *Chem. Mater.* **2011**, *23*, 4543–4547.
9. Novoselov, K. S.; Geim, A. K.; Morozov, S. V.; Jiang, D.; Zhang, Y.; Dubonos, S. V.; Grigorieva, I. V.; Firsov, A. A. Electric Field Effect in Atomically Thin Carbon Films. *Science* **2004**, *306*, 666–669.
10. Huang, P. Y.; Ruiz-Vargas, C. S.; van der Zande, A. M.; Whitney, W. S.; Levendorf, M. P.; Kevek, J. W.; Garg, S.; Alden, J. S.; Hustedt, C. J.; Zhu, Y.; *et al*. Grains and Grain Boundaries in Single Layer Graphene Atomic Patchwork Quilts. *Nature* **2011**, *469*, 389–392.
11. Robertson, A. W.; Bachmatiuk, A.; Wu, Y. A.; Schäffel, F.; Rellinghaus, B.; Büchner, B.; Rümmeli, M. H.; Warner, J. H. Atomic Structure of Interconnected Few Layer Graphene Domains. *ACS Nano* **2011**, *5*, 6610–6618.
12. Robertson, A. W.; Bachmatiuk, A.; Wu, Y. A.; Schäffel, F.; Büchner, B.; Rümmeli, M. H.; Warner, J. H. Structural Distortions in Few Layer Graphene Creases. *ACS Nano* **2011**, *5*, 9984–9991.
13. Han, G. H.; Gunes, F.; Bae, J. J.; Kim, E. S.; Chae, S. J.; Shin, H.-J.; Choi, J.-Y.; Pribat, D.; Lee, Y. H. Influence of Copper Morphology in Forming Nucleation Seeds for Graphene Growth. *Nano Lett.* **2011**, *11*, 4144–4148.
14. Luo, Z.; Lu, Y.; Singer, D. W.; Berck, M. E.; Somers, L. A.; Goldsmith, B. R.; Johnson, A. T. C. Effect of Substrate Roughness and Feedstock Concentration on Growth of Wafer-Scale Graphene at Atmospheric Pressure. *Chem. Mater.* **2011**, *23*, 1441–1447.
15. Wofford, J. M.; Nie, S.; McCarty, K. F.; Bartelt, N. C.; Dubon, O. D. Graphene Islands on Cu Foils: The Interplay between Shape, Orientation, and Defects. *Nano Lett.* **2010**, *10*, 4890–4896.
16. Vlassiouk, I.; Regmi, M.; Fulvio, P.; Dai, S.; Datskos, P.; Eres., G.; Smirnov, S. Role of Hydrogen in Chemical Vapor Deposition Growth of Large Single Crystal Graphene. *ACS Nano* **2011**, *5*, 6069–6076.
17. Ferrari, A. C.; Meyer, J. C.; Scardaci, V.; Casiraghi, C.; Lazzeri, M.; Mauri, F.; Piscanec, S.; Jiang, D.; Novoselov, K. S.; Roth, S.; Geim, A. K. Raman Spectrum of Graphene and Graphene Layers. *Phys. Rev. Lett.* **2006**, *97*, 187401.